Supporting Information

Freshwater-Electricity Co-Generation in Solar-Driven Water Desalination: An Effective Approach Towards Water-Energy Nexus

*Tawseef Ahmad Wani, Parul Garg, Priya Kaith, and Ashok Bera**

Department of Physics, Indian Institute of Technology Jammu, J & K, 181221, India

*Corresponding Author

Email Address: ashok.bera@iitjammu.ac.in

Note S1. Experimental Section/Methods

Materials: The SSA consisting of a cermet (ETA plus) coated on an aluminum sheet was provided by Alanod Solar, India. Sodium chloride, potassium hydroxide, sodium hydroxide, magnesium sulphate, and hydrochloric acid were purchased from Sigma-Aldrich. Whatman filter paper with a pore size of ~11 µm was used. All the chemicals were used without further purification.

Device fabrication: The cuboid-shaped evaporator with dimensions 1.5 cm × 1.5 cm × 2.5 cm / 5 cm was made from an SSA-coated aluminum sheet. To design the final device, the filter paper was cut into strips of length 8 cm / 10.5 cm which were attached to the walls of the cuboid by a stapler. The opposite end of the strips was dipped into the saltwater reservoir in such a way that the channel length between the upper electrode and the water surface remained between 3 to 4 cm.

Characterizations: Absorption spectra were measured in the range of 300 to 2500 nm using a UV-vis-NIR spectrometer (Cary-5000). The concentration of different ions was tracked by an atomic absorption spectrophotometer (AAS) (Shimadzu AA-6880 series).

Solar steam and electricity generation measurement: To measure the weight loss of the saltwater, the whole device was placed on an analytical balance (Mettler Toledo, ME204). The solar steam generation performance experiments were conducted using a AAA solar simulator (ABET 110005). The intensity of light was adjusted at 1000 W m^{-2} (1 sun) by a thermopile

sensor (Newport Corporation, 919P-003–10) connected with a light meter (Newport Corporation, 843-R). The source meter (Keithley 2450) was used to measure the generated voltages and the currents. All the experiments were performed at a room temperature of ~26 °C and relative humidity of ~ 55%.

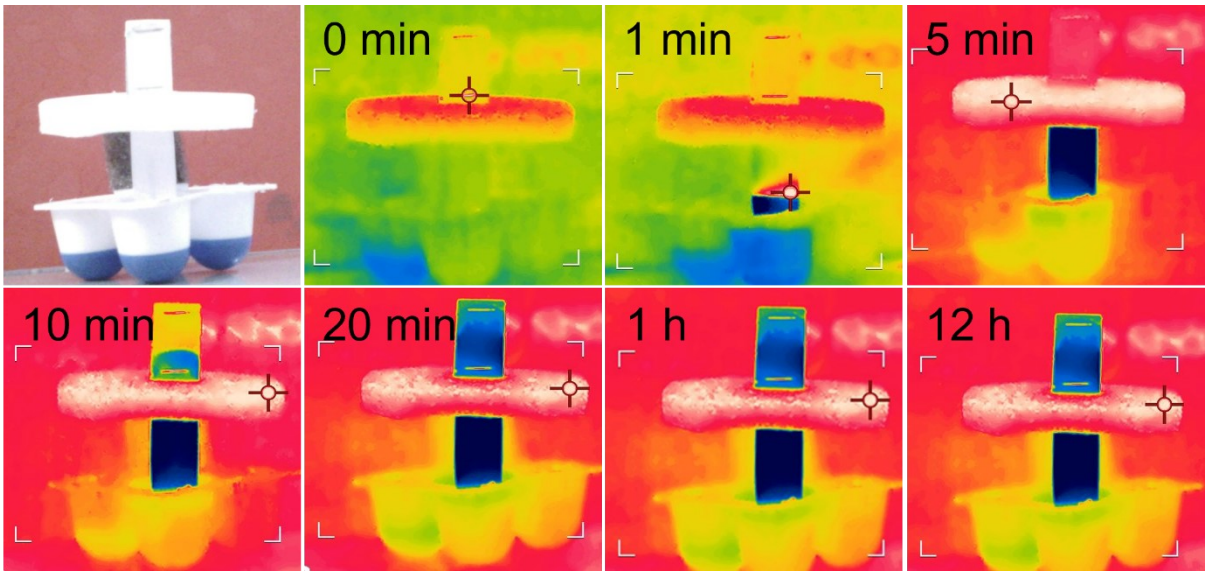

Fig. S1 The IR images taken at different times showing the water transport in the strip of filter paper through capillary force.

Note S2. Absorption calculations

To experimentally evaluate the light absorption performance, we measured the diffused reflectance of the cuboid-shaped SSA evaporator in the wavelength range of 300 to 2500 nm. The diffused reflectance due to the inner walls of the cuboid leads to high solar absorptance (α). The α was calculated using the following equation:

$$\alpha = \frac{\int_{300}^{2500} I(\lambda)(1 - R(\lambda))d\lambda}{\int_{300}^{2500} I(\lambda)d\lambda} \quad (1)$$

where λ is the wavelength, I(λ) is the light intensity function of the solar spectrum, and R(λ) is the reflectivity function of the cone at different wavelengths. The α value for the cone was calculated as 0.96.

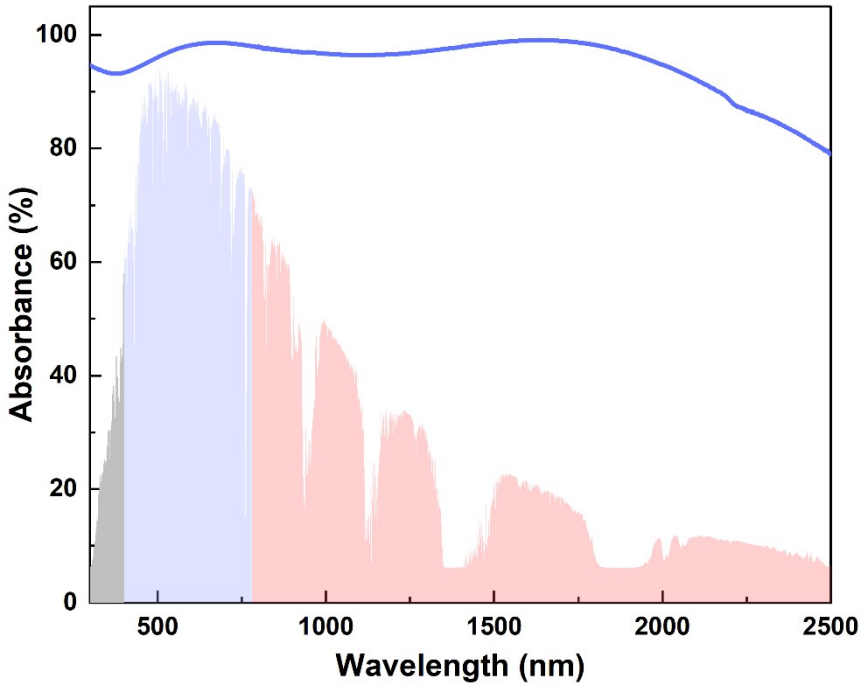

Fig. S2 UV-vis spectra of cuboid-shaped SSA-based evaporator.

Fig. S3 Photograph of the actual setup with the lower part covered with aluminum foil.

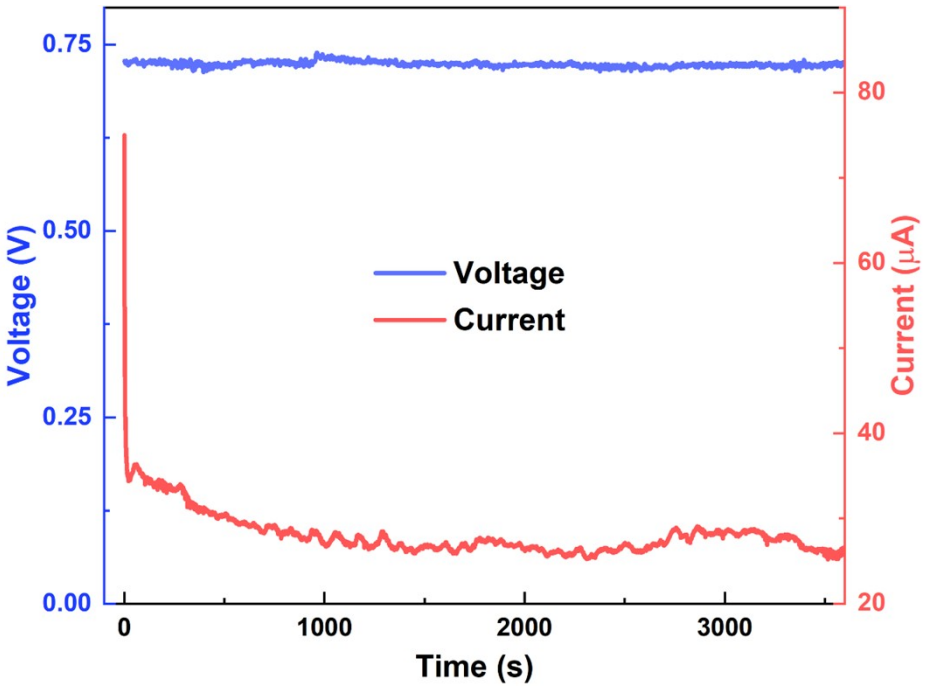

Fig. S4 Time response of V_{OC} and I_{SC} of a single strip.

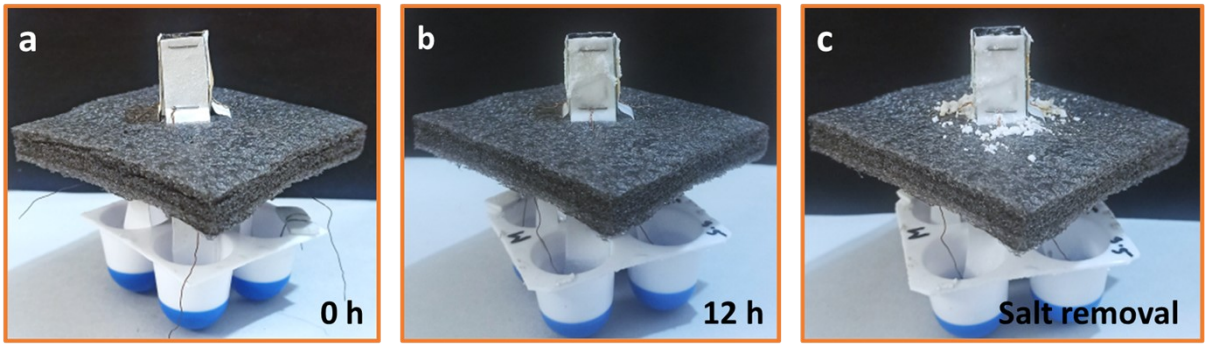

Fig. S5 Photos of the device showing the (a) pristine device before the start of the experiment, (b) salt accumulation after 12 h of operation, and (c) removal of accumulated salt.

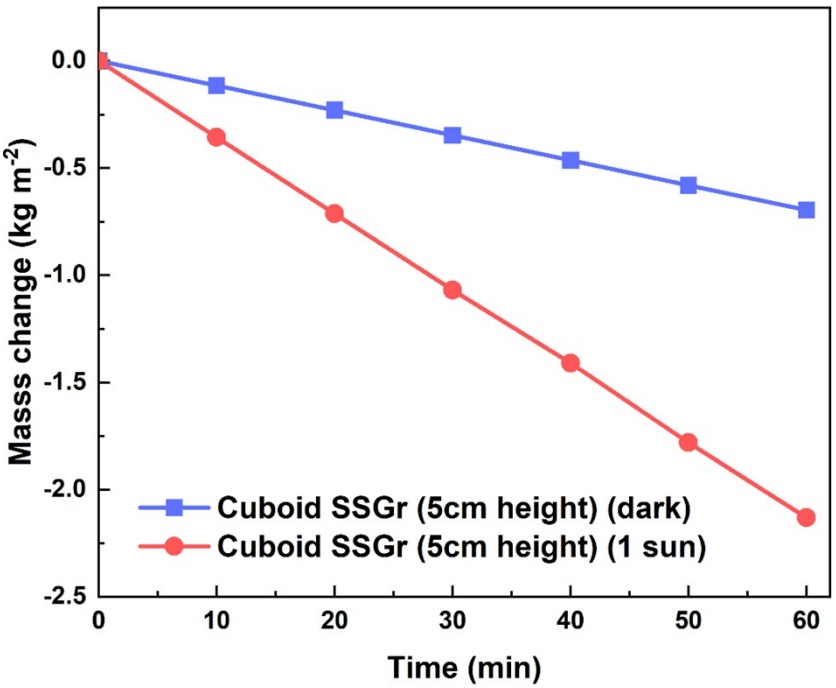

Fig. S6 Mass change of saltwater using a device of 5 cm height.

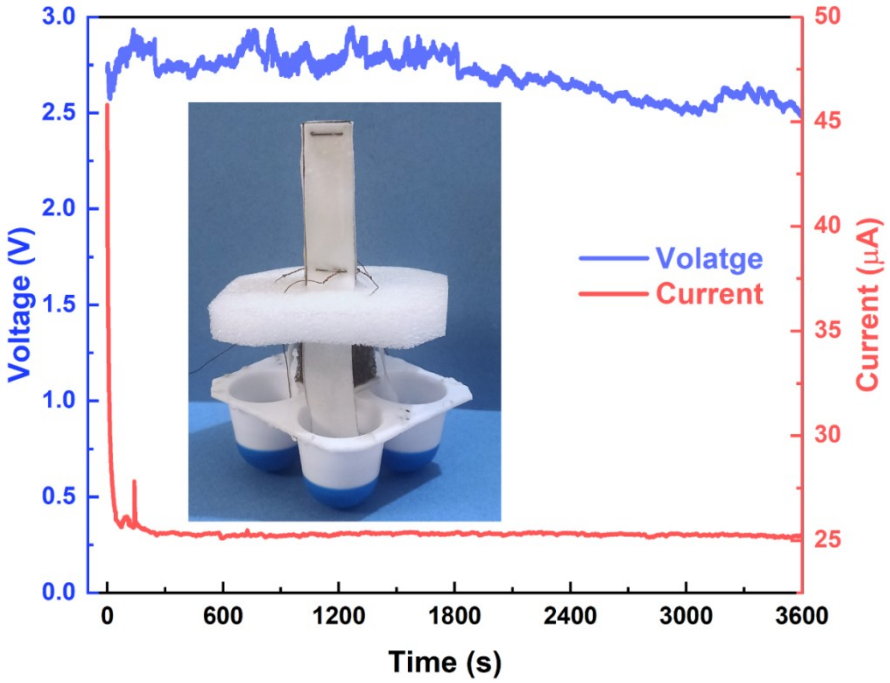

Fig. S7 Time response of V_{OC} and I_{SC} for the device of height 5 cm with all four strips connected in series.

Note S3: Mechanism of energy generation

When an ionic solution is pressed through the microchannels of filter paper, the streaming potential (V_S) is developed. The generation of electric potential is due to the accumulation of counter-charges (positive charges) due to the presence of negatively charged immobile ionic groups of within the material surface. Fig. S8a shows the formation of a static ionic double layer called a stern layer at the surface of the microchannels. To balance the surface-bound negative charge completely, more counter ions come close to the surface, forming a second layer called a diffuse layer in which the ions are loosely bound. When the fluid flows through the channel, the mobile part of the counter ions are dragged along the direction of flow, *Q*, caused by the pressure difference Δ*P* (originates from the strong adhesive force between filter paper and the liquid molecules) between the two ends giving rise to the generation of steaming current I_s (Fig. S8b) given as: [1,2]

$$I_S = \frac{A\varepsilon_0\varepsilon_r}{\eta l}\Delta P\zeta$$

where l and *A* are the cahnnel length (pore length) and cross-sectional area of the channel (pore), respectively. ζ is the zeta potential which measures the electric potential in the diffuse layer with respect to the bulk solution. ε_0, ε_r, and η are the permittivity of vacuum, the relative permittivity of the solution, and solution viscosity, respectively.

The attractive force on the positive charges creates charge polarization between the two ends. The charge polarization subsequently results in an electric field, *E*, which induces the ionic motion in the opposite direction, creating a current called a conduction current (I_C) given a:

$$I_C = \frac{A\sigma V_S}{l}$$

where σ is the ionic conductivity of the solution. At the equilibrium state (when $I_S + I_C = 0$), the V_S reaches its maximum value (Fig. S8c) given as

$$V_S = \frac{\varepsilon_0\varepsilon_r}{\sigma\eta}\Delta P\zeta$$

As we can see that the saturation voltage depends mainly on the physical properties of the filter paper and the ionic conductivity of the liquid, the saturation voltage is nearly independent of the flow rate. The variation in pressure gradient ΔP depends only on the difference in the cohesive force of the liquid molecules and the adhesive force between the filter paper and the molecules of the liquid.

It is to be noted that in the entire discussion, we have neglected the flow of negatively charged ions of the electrolytes. Ideally, the negatively charged ions can freely move along the mobile layers of each microchannel, resulting in their zero accumulation within the microchannel surface.

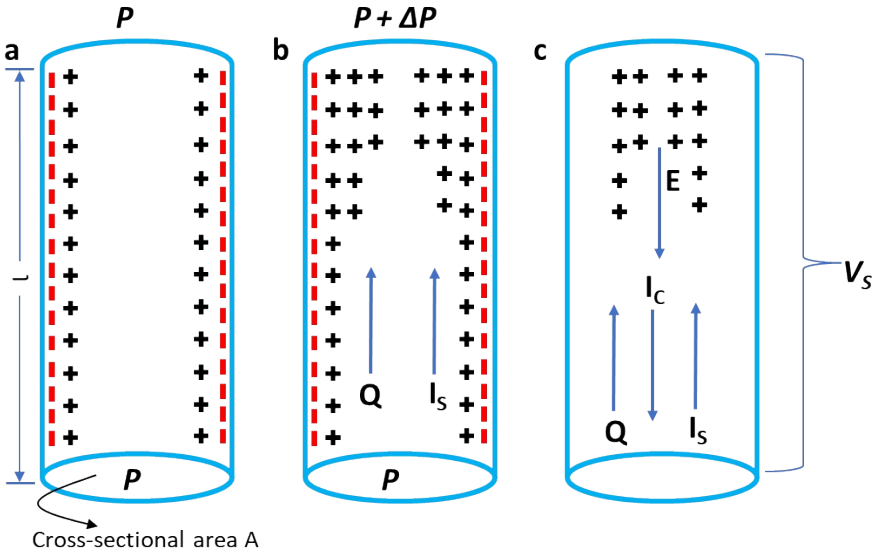

Fig. S8 (a) Drawing of a channel with pore length *l* and cross-sectional area *A* filled with the ionic solution, with negative charges on the surface forming the double layer with the counter ions present in the ionic solution. (b) The pressure difference between the two ends of a channel causes the generation of steaming current. (c) The charge polarization due to the flow creates an electric field and hence conduction current, which in turn creates the steaming potential.

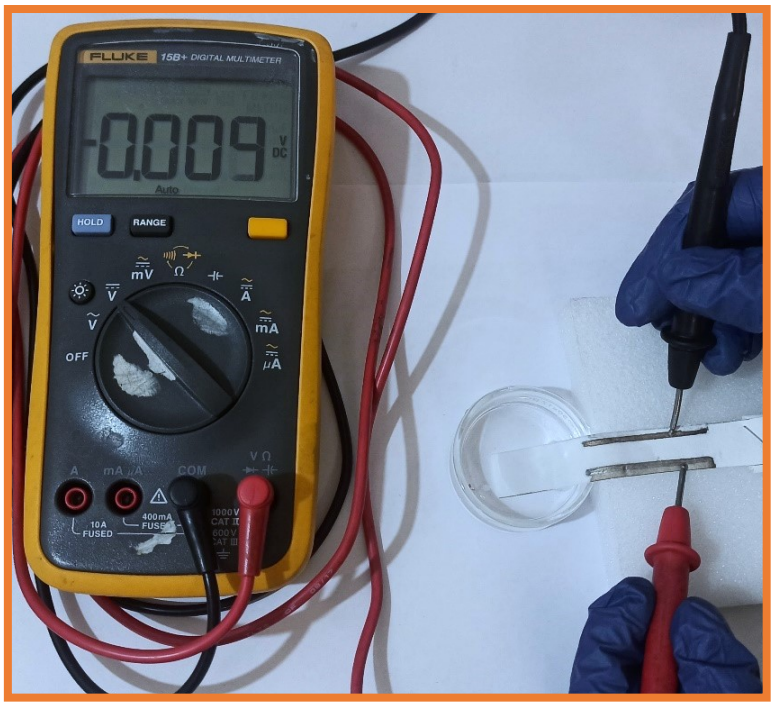

Fig. S9 Photograph of the voltage across the width of the strip.

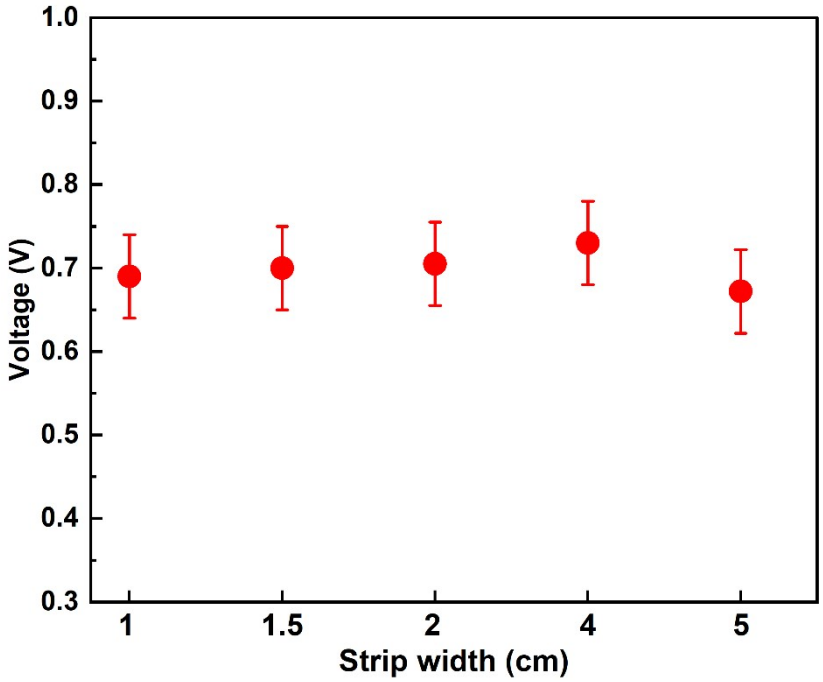

Fig. S10 Variation of the V_{OC} against different strip widths.

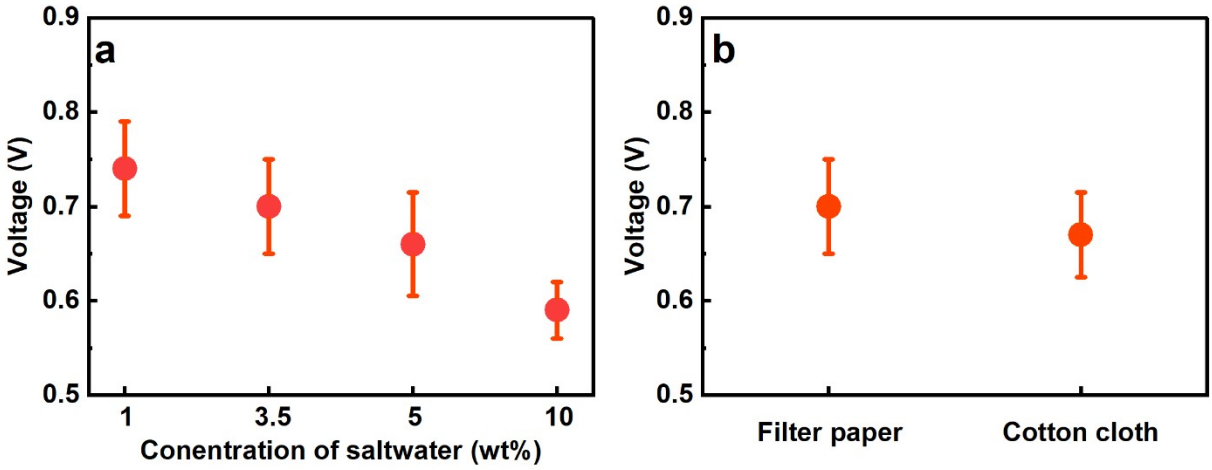

Fig. S11 Variation of the V_{OC} against (a) different saltwater concentrations and (b) different materials.

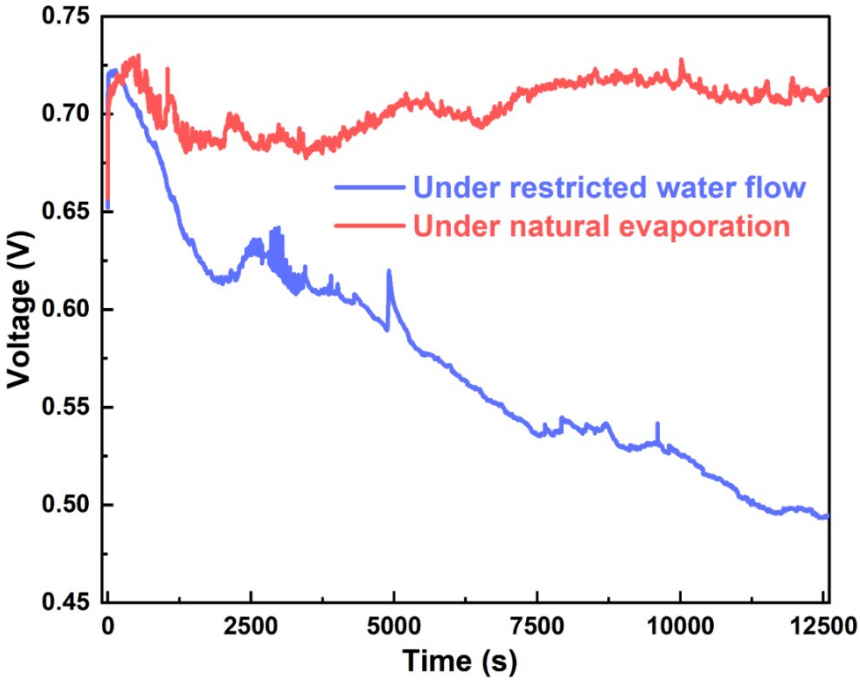

Fig. S12 Time response of V_{OC} for a single channel with and without taping the whole strip under natural evaporation.

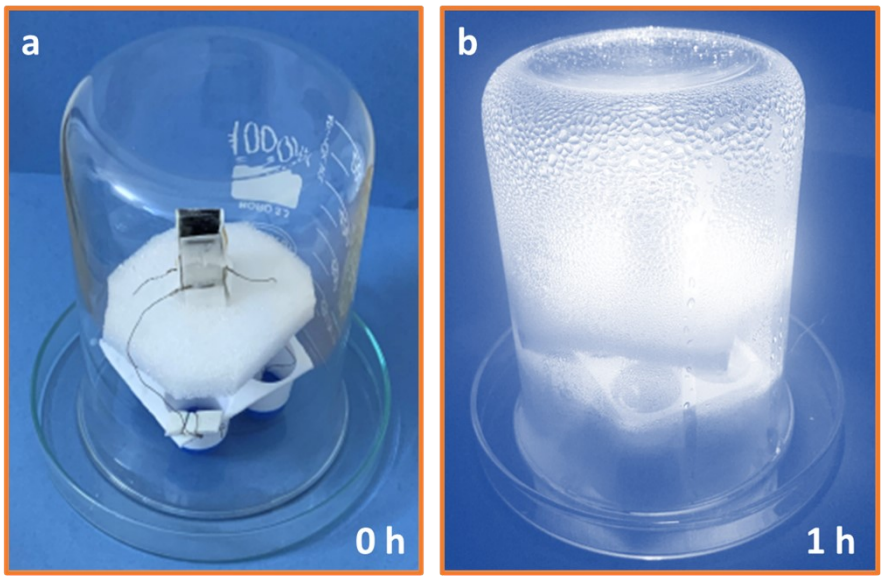

Fig. S13 Digital photos of vapor condensation after 1 h of light illumination.

References

1 W. Olthuis, B. Schippers, J. Eijkel and A. Van Den Berg, *Sensors Actuators, B Chem.*, 2005, **111**–**112**, 385–389.

2 A. T. Liu, G. Zhang, A. L. Cottrill, Y. Kunai, A. Kaplan, P. Liu, V. B. Koman and M. S. Strano, *Adv. Energy Mater.*, 2018, **8**, 1802212.